Differentiation and Localization of Ground RF Transmitters Through RSSI Measures from a UAV

SUBMISSION DATE / POSTED DATE

03-11-2023 / 09-11-2023

CITATION

Teeda, Vineeth; Moro, Stefano; Scazzoli, Davide; reggiani, Luca; Magarini, Maurizio (2023). Differentiation and Localization of Ground RF Transmitters Through RSSI Measures from a UAV. TechRxiv. Preprint. https://doi.org/10.36227/techrxiv.24494845.v1

DOI

10.36227/techrxiv.24494845.v1

Differentiation and Localization of Ground RF Transmitters Through RSSI Measures from a UAV

Vineeth Teeda, Stefano Moro, Davide Scazzoli, Luca Reggiani, Maurizio Magarini
Politecnico di Milano, Piazza Leonardo da Vinci, 32, 20133, Milano, Italy Politecnico di Milano, Italy. Email: (firstname.lastname)@polimi.it

***Abstract*—Low-altitude Unmanned Aerial Vehicles (UAVs) are a valuable solution for data gathering, surveillance, warfare, and mapping. In these applications, differentiating and estimating the position of ground Radio Frequency (RF) emitters is pivotal. To achieve this, we define an experimental setup based on Received Signal Strength Indicator (RSSI) collected by a single UAV at different points of a predefined trajectory. The experimental setup is evaluated for the two unlicensed frequency bands of $2.4\,\mathrm{GHz}$ and $865\,\mathrm{MHz}$ with and without interference, respectively. We show that the application of the maximum likelihood algorithm to the RSSI measures collected in experiments conducted in rural areas gives a mean absolute localization error of about $5\,\mathrm{m}$ and $4\,\mathrm{m}$ for a single transmitter with and without interference, respectively. A threshold-based technique is proposed to improve the accuracy in the presence of interference. For multiple transmitters, the RSSI data are divided into clusters and fed into a localization algorithm. A k-means clustering algorithm eliminates user intervention and identifies the number of RF emitters in the area. As a further contribution of the paper, we define an analysis phase where UAV flight path and data collection are simulated using the QuaDRiGa realistic radio impulse channel model.**

***Index Terms*—Unmanned Aerial Vehicles (UAVs), Received Signal Strength Indicator (RSSI), Software Defined Radio (SDR), GNU Radio, Localization, Interference, k-means clustering.**

I. Introduction

Unmanned aerial vehicles (UAVs) are expected to have a great impact in the telecommunications sector thanks to their unprecedented mobility. Their main envisaged uses are in search and rescue operations and in providing on-demand deployment of airborne base stations [1][1]. For such applications, the localization of ground targets from UAVs is often a useful feature and sometimes a necessary requirement [2], [3]. In search and rescue situations, re-establishing the connectivity with ground terminals and localizing them can save lives and expedite time-critical operations. In general, when speaking of target localization, it is possible to distinguish between *passive* or *active* localization; in the former, targets are often localized using radar, lidar, or other sensing technologies because they do not actively emit Radio Frequency (RF) signals while, in the latter case, they emit RF signals, which can be exploited to estimate their position [4].

Active localization of RF transmitters is a quite classical and well-studied problem in terrestrial and non-terrestrial wireless communication systems because the extensive availability of devices capable of measuring the Received Signal Strength Indicator (RSSI) [3], [5]–[8]. Many other approaches can be adopted to tackle the localization problem, i.e., Time of Arrival (ToA) [9], Time Difference of Arrival (TDoA) [10], and Angle of Arrival (AoA) [11], just to cite a few familiar techniques. However, it is important to observe that all these methods require more complicated or dedicated hardware than RSSI; therefore, RSSI localization is the most convenient choice in applications where devices are subject to tight constraints on their complexity, such as Wireless Sensor Network (WSN) [5], [8]. Regarding the specific problem of localization from UAVs, the crucial limitation is the weight of the payload. A UAV-based localization platform based solely on RSSI, or the difference of RSSI [12], may be therefore constructed with significantly simpler and lighter hardware compared to alternative approaches. However, the benefits of RSSI-based localization solutions come with the main drawback of measures that are biased due to errors in the UAV position and significantly more noisy due to path loss, shadowing attenuation, and fading of the signal.

Localization of RF Transmitters: Related Works

In recent years, researchers have looked closely at the use of UAVs to locate a ground-based RF transmitter. With the purpose of localizing the ground RF emitter, in [6] a UAV is employed as an anchor point in the localization process and its measurements are combined with those from the ground anchor nodes. In [7] a technique is discussed that uses three fixed-wing UAVs scanning together a large region of 10×10 km^2 and locating an unknown-power RF emitter. To the best of the authors' knowledge, there are no studies in the literature that address RSSI-based localization from a UAV in the presence of interference. These are mostly limited to indoor environments. Existing solutions use data collected from numerous directional antennas [13] or exploit the frequency hopping capabilities to avoid the interference [14]. A UAV-based wireless sensor network was simulated in [15], and compressed sensing was applied to RSSI for joint estimation of multiple emitters.

It is worth observing that only a few experimental works employ UAVs as anchor points, and among these, only a small number use RSSI-based localization. In [8], multiple ground anchor nodes based on ZigBee transceivers are deployed as part of the localization of RF emitters on the ground. Other

[1]This paper is an extension of the conference paper, Moro, Stefano, et al. "Experimental UAV-Aided RSSI Localization of a Ground RF Emitter in 865 MHz and 2.4 GHz Bands." 2022 IEEE 95th Vehicular Technology Conference:(VTC2022-Spring). IEEE, 2022.

approaches present in the literature use the UAV to gather data and learn how to maneuver it [16], [17]. In [16], it is shown how to locate and move a UAV toward a ground RF emitter by comparing the RSSI from the two antennas mounted at the front and rear. In [17], many directional antennas onboard a UAV are connected to a single receiver through a switch to sense the power and allow for a fast estimation of the ground RF transmitter bearing.

Contributions

In this work, we propose an experimental setup where a Raspberry Pi board coupled with an Adalm Pluto Software Defined Radio (SDR) RF module collects RSSI values using a single omnidirectional antenna [18]. RSSI data in the $2.4\,\text{GHz}$ Industrial Scientific Medical (ISM) band are collected using different UAV trajectories. Furthermore, a baseline localization algorithm based on multi-lateration is provided. For the localization of the ground RF emitters, the gathered data are processed by a Maximum Likelihood (ML) algorithm. At the same time, local WiFi access points or the remote control may occasionally cause irregular interference at $2.4\,\text{GHz}$, which can reduce localization accuracy. The impact of WiFi interference is taken into account and a threshold-based solution is defined to mitigate its impact on RSSI ranging. Differently from the interference management approach in [13], this work does not require directional antennas and additional hardware, so reducing the weight and complexity of UAV operations. Then, the $865\,\text{MHz}$ spectrum is also considered for the accuracy validation without significant interference. The localization performance in this band is also illustrated by a series of flights.

The initial feasibility study of the proposed UAV-based localization approach was done by simulation using the QuaDRiGa channel model [19]. QuaDRiGa enables the testing with simulated channels with characteristics that are very close to those met in real scenarios. The developed simulator represents a useful tool for the prior assessment of the performance of the proposed localization platform considering different UAV trajectories [20]–[22].

The proposed approach has been evaluated both considering single and multiple ground RF emitters. In order to estimate their number, we have resorted to the use of k-means clustering method. Recently, machine-learning approaches have been widely explored and used in many fields. In localization technology, machine learning is often used to classify a large number of characteristic parameters of wireless signals from user devices in order to improve localization accuracy. They are mostly employed in indoor scenarios based on fingerprinting [23]–[26]. In [27] it simulates the use of a k-means clustering algorithm for detecting the presence of multiple transmitters via UAV-based mapping; a three-dimensional (3D) contour plot is built using measured power, and machine learning algorithms are used to estimate the positions of the transmitters. Here, we solve the issue of identifying the number of ground RF transmitters when applying the localization algorithm. Initially, the k-means clustering algorithm was adapted to identify the number of transmitters corresponding to the number of identified clusters and to divide the data for the localization algorithm into the respective clusters. Then the centroids of the identified clusters are considered as the estimates of transmitters' positions. Simulations employing the QuaDRiGa channel model have also been used to develop and test the k-means algorithm before practical trials.

The main new contributions of this paper, which is an extension of our previous work [1], can be summarized as follows:

- Definition of a UAV platform and experimental validation of an RSSI-based localization algorithm of RF ground emitters at $2.4\,\text{GHz}$ and $865\,\text{MHz}$.
- QuaDRiGa channel model simulations to define and test scenarios close to realistic conditions.
- Evaluation of the impact of interference from WiFi sources and development of a threshold-based approach for its mitigation.
- Identification and localization of multiple RF ground transmitters based on the k-means clustering and experimental validation.

Compared to [1] new scenarios have been investigated, tested, and experimentally evaluated.

Organization of the Paper

The rest of the paper is organized as follows: Sec. II introduces the scenario focusing on the path loss model, the threshold-based interference mitigation, the ML localization algorithm, and the k-means clustering algorithm. MATLAB simulations reporting the performance obtained using the QuaDRiGa channel model are reported in Sec. III. Then Sec. IV describes the measurement campaign for gathering real RSSI values, including the UAV path control. Sec. V presents the localization results concerning single and multiple RF ground transmitters. Finally, Sec. VI concludes the paper and discusses future work.

II. System model

A. Path Loss Model

The signal attenuation is related to the RSSI through the path loss model, expressed in the logarithmic domain [28]. In this relation, the inaccuracy is mainly due to the shadowing impact, which increases linearly with the distance (as shadowing introduces a constant error in the log-distance relation), and to the multipath (particularly for indoor scenarios), where RSSI fluctuations cannot be predicted by deterministic models. Thus, the measured power at the distance $d\,\text{m}$ can be expressed as

$$P_r(\text{dBm}) = P_{\text{ref}}(\text{dBm}) - n_p \cdot 10\log_{10}\left(\frac{d}{d_{\text{ref}}}\right) + n, \quad (1)$$

where P_{ref} is the power received at the reference distance of $d_{\text{ref}}\,\text{m}$, n_p is the path loss exponent, and n is the random shadowing component, which is Gaussian with zero mean (in dB). This model is adapted to the experimental scenario by setting n_p; in addition, due to the absence of large structures such as buildings or trees, the channel model that fits best this experimental scenario is the two-ray ground reflection and this is validated by the real measurements on the field.

Fig. 1: Experimental setup of the ground-to-air link. There are two ADALM-Pluto SDRs on the roof of a car: one is the transmitter and the other is used for monitoring.

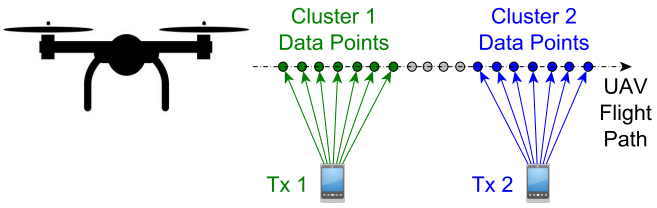

Fig. 2: Data points clustering approach in the presence of two transmitters.

B. Maximum Likelihood Estimation of the Ground RF Emitter

The ML algorithm uses the collected data to estimate the parameters of a given distribution by maximizing the likelihood function [29]. In the considered scenario, each UAV position defines an Anchor Point (AP). Let $\mathbf{u}$ and $\mathbf{s}_i$ be the 3D state vectors that give the coordinates of the active RF emitter and of the UAV associated with the ith RSSI measure, respectively. A single RSSI measurement ρ_i at position $\mathbf{s}_i$ is modelled as [30]

$$\rho_i = h_i(\mathbf{u}, \mathbf{s}_i) + n_i, \quad i = 1, \ldots, N_{AP}, \tag{2}$$

where N_{AP} is the number of APs, n_i is the zero-mean additive white Gaussian noise with standard deviation σ_i, and

$$h_i(\mathbf{u}, \mathbf{s}_i) = P_{\text{ref}} - n_p \cdot 10 \log_{10} \frac{\|\mathbf{u} - \mathbf{s}_i\|}{d_{\text{ref}}} \tag{3}$$

is a non-linear function of the state vectors ($\mathbf{u}$,$\mathbf{s}_i$) obtained from (1) with $d = \|\mathbf{u} - \mathbf{s}_i\|$, being $\|\mathbf{v}\|$ the norm of the vector $\mathbf{v}$. The ML estimate of the position of the ground RF emitter $\hat{\mathbf{u}}$ is obtained from the set of measurements in (3) as

$$\hat{\mathbf{u}}_{\mathbf{ML}} = \arg\max_{\mathbf{u}} \prod_{i=1}^{N_{AP}} \frac{1}{\sqrt{2\pi(\sigma_i)^2}} e^{-\left(\frac{\rho_i - h_i(\mathbf{u}, \mathbf{s}_i)}{2\sigma_i}\right)^2}. \tag{4}$$

The absolute error is calculated as the distance between the true position of the transmitter and the ML estimation.

C. Threshold-based Approach for Data Processing

In order to improve the accuracy of the ML localization algorithm, a pre-processing phase can refine the raw data and reduce the impact of noise and interference [31]. In this paper, the definition of the lower and upper thresholds makes the data usable and increases the algorithm's efficiency. For the initial measurements, the UAV is close to the transmitter, as shown on the car roof in Fig. 1, and there is also some interference due to the persons before the takeoff and multipath reflections. Hence, the measurements when the UAV is close to the transmitter are neglected, and an upper threshold of $-50\,\text{dB}$ is used to this aim. At the same time, RSSI measurements lower than a certain value are discarded as they are comparable to the SDR noise floor. These lower and upper thresholds were derived empirically from the measures will be presented in Sec. V.

D. k-means Clustering Algorithm

Clustering is one of the most established unsupervised learning techniques in machine learning. One of the most prominent clustering algorithms is k-means, where the goal is to divide the data into k clusters [32]. In our approach, this translates to clustering data points collected during the UAV flight, as shown in Fig. 2. These clusters are useful to distinguish multiple transmitters and their relative centroids can be used directly as an estimate of the transmitters' positions. A centroid is the center of the cluster, at which the sum of distances from all the data points that belong to that cluster is minimum. In order to evaluate the appropriate number of clusters, the elbow method is used [33]: the algorithm is run several times with an increment in K and records Within cluster the Sum of Squares (WSS), which measures the distance from the centroid of the points belonging to that cluster.

In a D-dimensional space, let us consider N sets of points represented by a $N \times D$ data matrix $\mathbf{X}$. Each row of $\mathbf{X}$ represents a single point. Initially, the k-means algorithm assigns randomly k cluster centroids, which can be represented by a $k \times D$ centroid matrix $\mathbf{C}$. For each iteration, each point is assigned to the closest cluster centroid by calculating the squared Euclidean distance. Then, the centroid of each cluster is recalculated by averaging all the coordinates of the points belonging to that cluster. These steps are repeated until k_{max} (specified by the user) is reached or until the WSS no longer decreases. The optimal k is chosen when the WSS curve starts to bend and converge, which is also known as the elbow point.

III. QuaDRiGa Simulations

Prior to the experimental campaign, the QuaDRiGa channel model was used to evaluate the feasibility of the proposed hardware setup by simulating the UAV flight path in the presence of RF emitters. The Non-terrestrial Network rural Line-of-Sight (NTN Rural LoS) scenario was considered to introduce realistic parameters in the propagation model, which are consistent with the experimental campaigns. Parameters such as velocity, altitude, flight time, flight path, and receiver

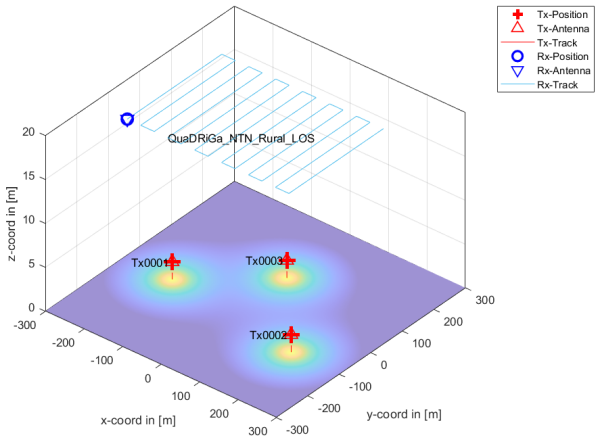

Fig. 3: QuaDRiGa Rural LoS simulation with 3 emitters.

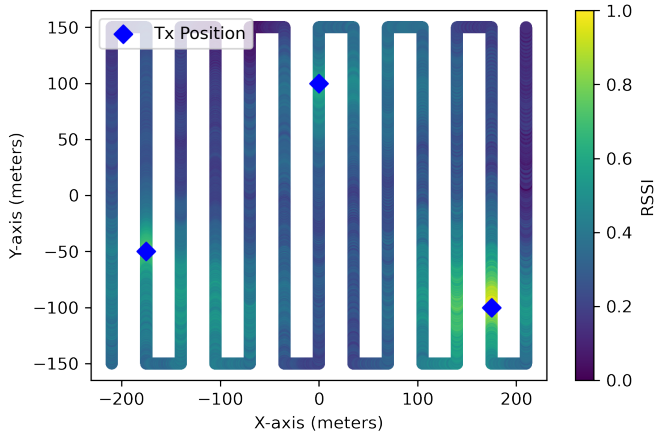

Fig. 4: QuaDRiGa simulated track with RSSI as gradient.

antenna array on UAVs were introduced based on specifications from the commercially available UAVs. Afterward, the number of RF emitters, their position, and antenna array are defined as parameters of our simulations. Once the scenario is established, the simulation yields RSSI coupled with the UAV positions. An example of a QuaDRiGa simulation in MATLAB with three emitters and a UAV track is shown in Fig. 3.

The data obtained using the Rural LoS simulation after min-max normalization are shown in Fig. 4 with RSSI illustrated by the gradient. Once the cutoff of RSSI < -90 dB is applied, the darker points in the track are cleared out. Then data are fed into the k-means clustering algorithm to identify the number of transmitters and to partition the data. The elbow graph in Fig. 5 shows that at $k=3$ the WSS starts to diminish. The clusters formed along with the simulated track are shown in Fig. 6. Then, the same parameters were used in the Urban LoS scenario, and the WSS starts to diminish at $k=3$ as shown in Fig. 5. The final clustering, along with the estimate of the transmitter's position, is shown in Fig. 7.

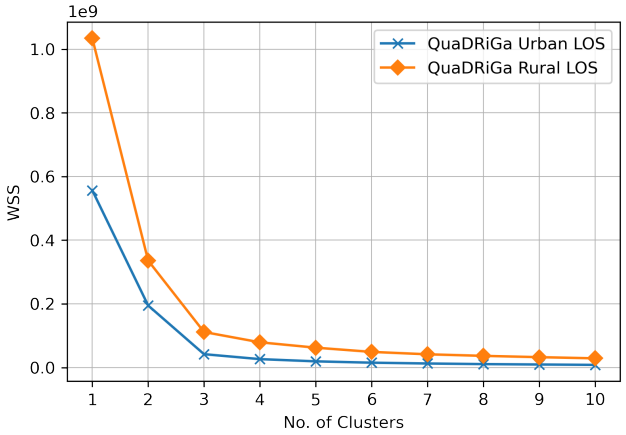

Fig. 5: Elbow Plot - QuaDRiGa Rural and Urban LoS simulation.

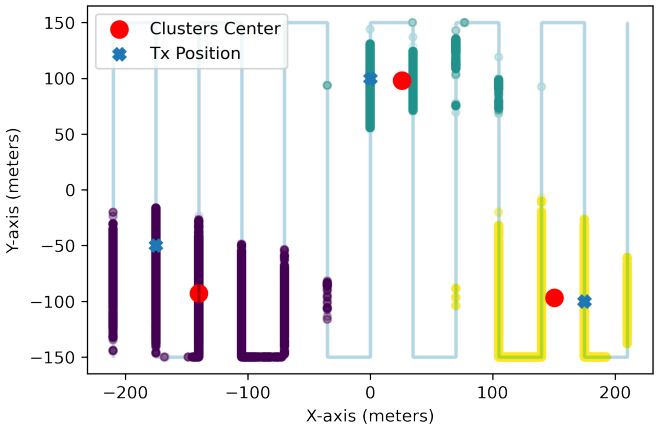

Fig. 6: k-means output - QuaDRiGa NTN Rural LoS.

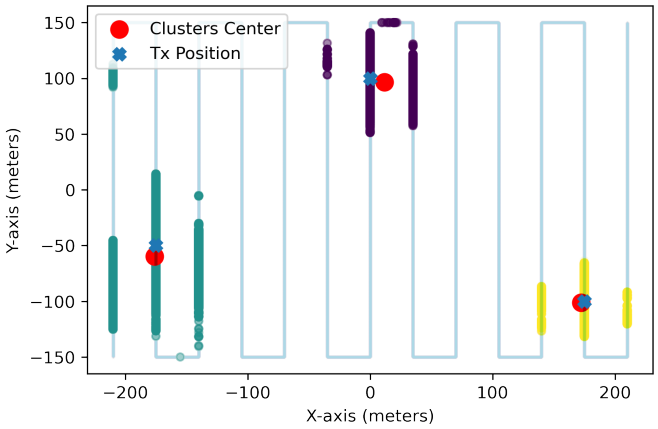

Fig. 7: k-means output - QuaDRiGa NTN Urban LoS.

IV. Experimental Measurement Campaign

The experimental setup used in this study was designed to be simple and efficient. The ground segment involved an ADALM-Pluto SDR [18], which is lightweight and has a wide frequency range for both single and multiple emitter scenarios. The ADALM-Pluto SDR allowed experimental campaigns

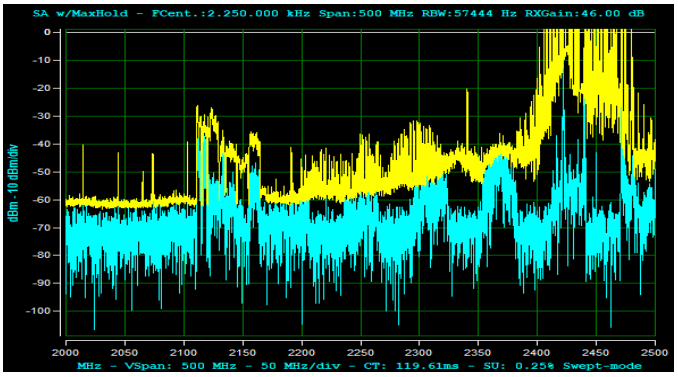

Fig. 8: The light blue signal is the UAV controller transmission at 2.4 GHz and the yellow one is the max-hold of the received power. The frequency-hopping nature of the transmission is the main cause of interference.

Fig. 9: Transmitter setup in multiple emitters scenario.

Fig. 10: The Tarot UAV in its complete configuration: the ADALM Pluto SDR as RF front end and the Raspberry Pi with the SenseHat IMU board for data logging.

Fig. 11: The flight track of the UAV was predetermined before the flight. We used a serpentine-like pattern to cover the designated area.

both in the 865 MHz [34] and 2.4 GHz frequency bands. The emitter setup for the standalone scenario depicted in Fig. 1 was described in detail in [1], which involved transmission of a QPSK-modulated signal at a carrier frequency of $f_c = 865$ MHz without interference and $f_c = 2.4$ GHz with interference. The source of interference in the experimental campaign was a WiFi hotspot and the UAV controller, as shown by Fig. 8. As both frequencies are part of the unlicensed spectrum, signals were transmitted with the maximum power of the SDR, which is 7 dBm. In the multiple emitter scenario, each emitter included an ADALM-Pluto SDR running a MATLAB script paired with a power bank, as shown in Fig. 9; we took advantage of the *transmit and repeat* mode available in the MATLAB API, which allowed us to load the waveform samples in the internal memory of the SDR and transmit them continuously. This setup allowed the SDR to emit constantly a QAM-modulated signal without the need for an external computer.

The receiver component of the setup involved an identical SDR paired with a Raspberry Pi 3B on the UAV, as depicted in Fig. 10. The RSSI values were recorded using the GNURadio application with 10 ms sampling time. This sampling time of the RSSI signal is easily achievable also with a low-cost transceiver [35]. The transceiver AD9361 used in the setup measures the dB power level and compensates for the receiver gain in order to provide the RSSI value. For this reason, we could take advantage of the Adaptive Gain Control (AGC) system on the board to face near and far-range situations without manually changing the receiver gain value. However, the RSSI value returned by the board is not calibrated but is only a relative value. Therefore, a calibration measure at a distance of 1 m was used to estimate the values of all the gains at the receiver and match the relative RSSI measures to the actual path loss values. Overall, the experimental setup turned out to be effective in collecting the necessary data to evaluate the performance of the k-means clustering algorithm and localize an active RF transmitter.

A. UAV Path Control

Localizing a ground RF emitter using UAVs involves several key steps, and defining the flight path is one of the fundamental aspects. Several path planning algorithms have been developed to optimize the path and ensure accurate localization, such as the one reported in [36]. This particular algorithm defines a set of way points on a circular path covering the target area.

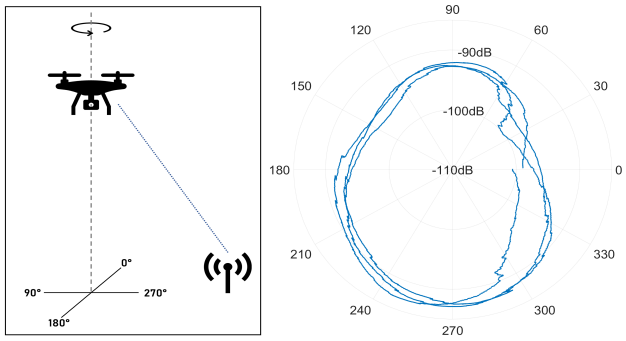

Fig. 12: The RSSIs collected by the UAV while rotating around its vertical axis are presented in polar form. The graph shows a clear relationship between the change in the UAV bearing and the RSSI values. The variation in the RSSI can be attributed to the shadowing effect caused by the UAV.

The circle radius is a crucial parameter, as it should be large enough to cover all possible target locations while minimizing battery usage. Another approach studied in [37] relies on a Reinforcement Learning (RL) algorithm to dynamically define a trajectory that minimizes the error in the localization. In this work, it has been simulated a double-phase approach where firstly, the UAV has to scan the complete area and then fly with an RL-based trajectory.

In our experimental activity, we prioritized a fast and simple setup deployment. Therefore, to evaluate the effectiveness of the path-planning algorithm, we conducted a series of experiments using both programmed and manual flight paths. The programmed flight path followed a serpentine and Ulam spiral pattern to keep the UAV tilt angle low and minimize potential interference with the RF emitters. The UAV was moved at a controlled speed between 2 and 3 m/s, and the RSSI measuring interval was set to 10 ms, which corresponds to a spatial interval $\Delta d = 2.3$ cm. These parameters allowed for a high spatial sampling frequency, enabling an effective averaging of the measurements. We verified that the path planning algorithm used in this study localized the ground RF emitters effectively with good accuracy, as shown in Sec. III.

B. UAV Trajectory Estimation

Accessing UAV flight telemetry can be challenging, especially during a flight when the log file stored in the UAV may not be available. To overcome this issue, we utilized an external add-on board mounted on the drone to acquire attitude and position data. Regarding the attitude data, we chose an Inertial Measuring Unit (IMU) board that can collect pitch, yaw, and roll angles using an accelerometer, a gyroscope, and a compass [38]. Although the sensor returned noisy measurements, we were still able to obtain a realistic representation of the UAV attitude. Fig. 12 shows the effect of the UAV bearing on the measured RSSI.

By rotating the UAV away from the transmitter, we experience an instantaneous fading in the received power, which follows the trend of the yaw measure. This data was useful for the localization algorithm since we could compute the exact directivity of the onboard antenna and weigh each collected RSSI sample. It is important to notice that all the attitude data provided by the IMU board are relative angles w.r.t. the orientation at the startup time. An external GPS dongle [39] was used to evaluate 2D positions of the UAV. The position accuracy of the 2D estimate is around 2.5 m and depends on the number of visible satellites at the time of the trial. This framework is further detailed in [1].

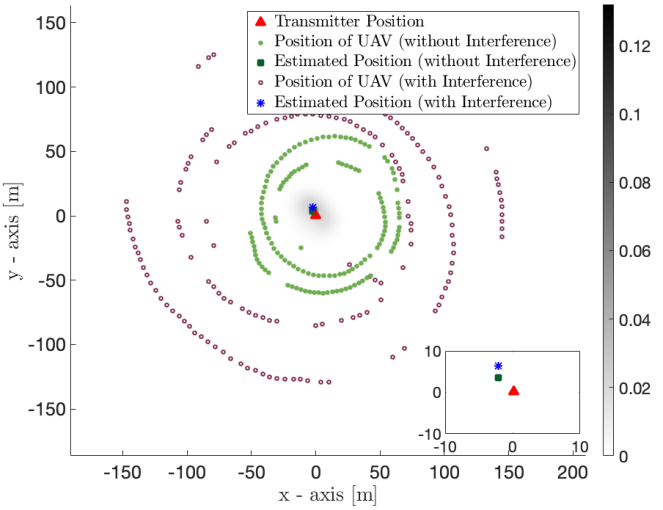

Fig. 13: ML estimation of the transmitter position with and w/o interference for the shown circular UAV flights.

V. Localization Results

In this section, the estimation of the emitters' positions by means of the ML localization and k-means clustering algorithms is presented and discussed. In the case of a single emitter, a traditional ML localization algorithm is used, and the results in the absence and presence of interference at 865 MHz, and 2.4 GHz are presented. The channel is essentially a two-ray model, i.e. LoS plus a reflection from the ground, as the emitter is located on the rooftop of a car. Hence, $n_p = 2.2$ was used in (1), and it was verified empirically. RSSI is sampled and recorded each 10 ms while the position update rate is twice per second. The standard deviation σ_i used in (4) varies between 2 and 6 dB, and it was estimated by calculating the mean value of the measurements taken at a reference position. For mitigating the presence of interference and low reliability of the RSSI measure, only a subset has been considered, i.e. data derived from the application of the threshold-based approach (Sec. II.B).

The position estimate of the emitter is reported in Fig. 13. Two scenarios with and without interference using circular tracks are shown. Here, the same value $\hat{\sigma}_i = 4$ dB, $i = 1, \ldots, N_{AP}$, was used in (4), since it was selected as a median of the standard deviation values observed from the collected RSSIs. The green and gray points in the figure represent the UAV APs considered for the localization after the threshold-based approach. The likelihood of the estimated positions of the target is reported on the right of the figure. Here, a mean absolute error of 4 m is obtained in the absence of interference, while it increases to 4.8 m with interference. Notably, interference degrades the estimate by less than a

TABLE I: RSSI range (thresholds) and mean absolute position error for circular and serpentine tracks.

RSSI Thresholds (upper and lower)	Mean Absolute Position Error			
	Circ. w\Int.	Serp. w\Int.	Circ. No Int.	Serp. No Int.
-50 to -90 dBm	7 m	17 m	5.1 m	11.3 m
-50 to -95 dBm	5.5 m	14 m	4.1 m	16.4 m
-50 to -100 dBm	7.2 m	19 m	9.5 m	17.0 m
-50 to -105 dBm	10.8 m	14 m	12.2 m	16.5 m
-60 to -90 dBm	6.7 m	17.7 m	5.1 m	10.2 m
-70 to -90 dBm	6.1 m	16.7 m	5.1 m	16.4 m
-70 to -100 dBm	7.1 m	10.5 m	9.4 m	17.1 m
-70 to -110 dBm	12.9 m	13.2 m	12.3 m	16.2 m

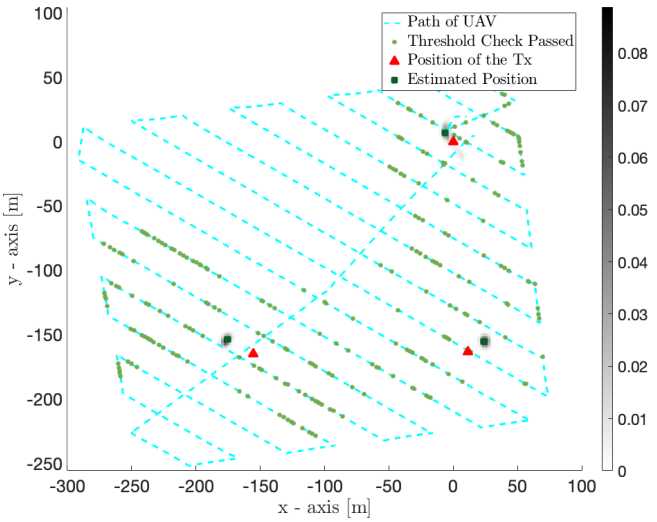

Fig. 14: Multiple transmitters position estimation using ML algorithm with a serpentine track.

meter. The summary of the results obtained with different RSSI thresholds in multiple experimental tests for circular and serpentine tracks (Fig. 11) is reported in Table I. It is clear that (i) the interference does not affect the position estimate significantly and (ii) a circular track is generally better for localization as there are measurements from all directions.

A. Multiple Transmitters

In order to verify the performance of the experimental setup and ML algorithm in the presence of multiple transmitters, measures were collected in an area of $300 \times 300\,\mathrm{m}^2$ in the presence of 3 transmitters. A serpentine and an Ulam spiral track were pre-programmed for the UAV, lasting 15 minutes and 8 minutes respectively. Data were divided into 3 clusters followed by the analysis of RSSI measures and detection of the hot spots in the UAV track, suggesting the presence of a transmitter on the ground. In both cases, $\hat{\sigma}_i = 6\,\mathrm{dB}$ was chosen after observing the standard deviation in the raw RSSI data. Then, the localization procedure is applied in the 3 clusters independently, and the results are merged. Fig. 14 shows the estimated positions returned by the ML algorithm in the serpentine track while those obtained with the Ulam spiral track are shown in Fig. 15. The mean absolute errors in both the scenarios are reported in Table II. We can observe that the estimation is worse in the case of a spiral track as

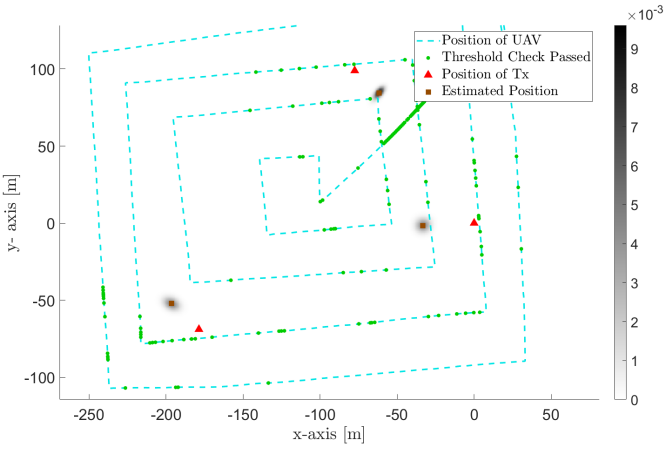

Fig. 15: Multiple transmitters position estimation using ML algorithm with a Ulam spiral track

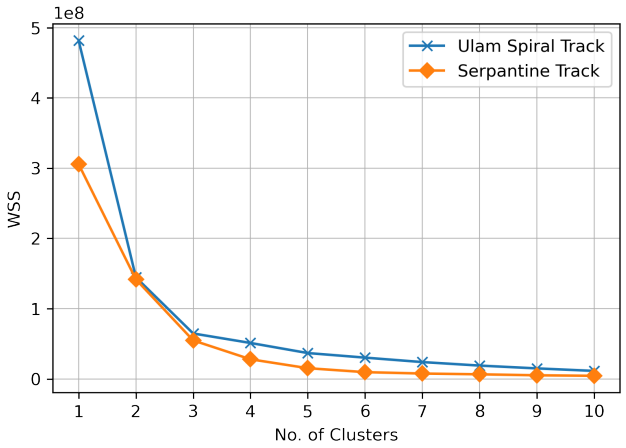

Fig. 16: Elbow plot to determine the number of transmitters.

this track is not dense enough and not enough measures are collected to estimate accurately the final position.

Now, moving to the localization of multiple emitters using the k-means clustering algorithm, we can observe that in the case of the serpentine track, the algorithm was able to divide the data into clusters equal to the number of transmitters present and the corresponding elbow plot is presented in Fig. 16. The symbol k is the number of clusters on the x-axis and the plot starts to converge at $k = 3$. The final output of the clustering algorithm, along with the centroids, is presented in Fig. 17. Assuming the centroids of the clusters as estimates of transmitters' positions and comparing them with Fig. 14, we observe that the k-means clustering algorithm performs slightly better than the ML localization algorithm. It is worth mentioning that the k-means algorithm requires very limited computing power and time compared to ML localization. Now, feeding the data from the Ulam spiral track into the k-means clustering algorithm, the resulting elbow plot is depicted in Fig. 16. Similarly to the serpentine track, the elbow plot starts to converge at $k = 3$ and the final estimates of transmitters, i.e. centroids along with respective clusters, are shown in Fig. 18. The mean absolute errors obtained

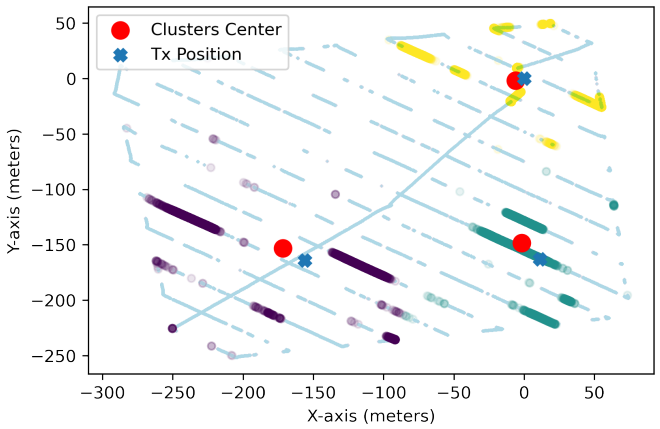

Fig. 17: k-means output - Serpentine Track

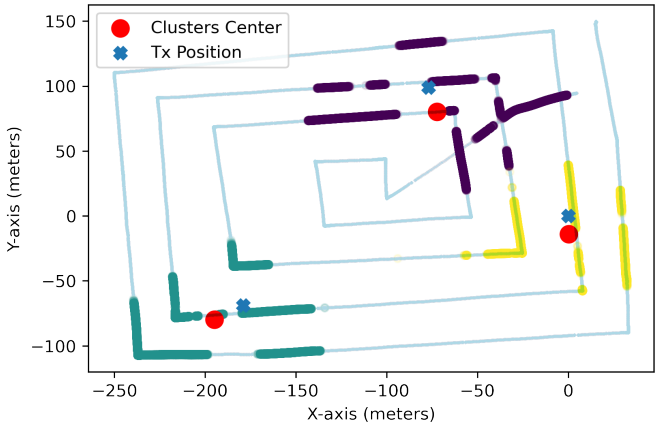

Fig. 18: k-means output - Ulam Spiral Track

TABLE II: Mean absolute error of ML and k-means estimates for the 3 transmitters.

UAV Track	ML algorithm	k-means Clustering
Serpentine	(25, 11, 15) m	(20, 6.1, 19) m
Ulam Spiral	(33, 24, 22) m	(14, 19.4, 19) m

using the k-means algorithm in both scenarios are reported in Table II: the differentiation and position estimation of the multiple transmitters using the Ulam spiral track turns out to be equivalent to the serpentine track. This latter saves UAV flying time by about 40 percent and gives a decent estimate of the positions of the transmitters.

VI. Conclusions and Future Work

In this paper, we considered the utilization of Maximum Likelihood localization algorithm and k-means clustering algorithm for estimating the positions and the number of active RF transmitters from RSSI measures collected by a UAV in two unlicensed frequency bands. An experimental setup that uses an inexpensive and lightweight ADALM Pluto SDR development board programmed with open-source software GNU Radio was described. Circular, serpentine, and Ulam spiral tracks have been considered as trajectories for the UAV in the experimental data collection campaign. Performance has been evaluated in terms of mean absolute position error either without interference at 865 MHz or with interference at 2.4 GHz. A threshold-based solution on the measured RSSI inputs has been proposed to improve the accuracy of the estimates. Our results show that the performance in the presence of interference at 2.4 GHz is comparable to the scenario without interference at 865 MHz. The applicability of this approach to a multi-transmitter case has been demonstrated for a scenario with three RF emitters, in which good accuracy is achieved. It is shown that using k-means clustering algorithm provides a more efficient localization in terms of consumed energy and computational requirements.

This work can be extended in the future to more complex environments. The data collection campaign can be extended to allow the training of more complex machine learning algorithms. Finally, the setup can be extended by introducing user feedback based on real-time measures or autonomous UAV path planning in order to maximize localization accuracy.

VII. Acknowledgements

This project was partly funded by NATO-SPS funding grant agreement No. G5482. The work of M. Magarini was supported by the European Union under the Italian National Recovery and Resilience Plan (NRRP) of NextGenerationEU, partnership on “Telecommunications of the Future” (PE00000001 - program “RESTART”, Structural Project 6GWINET).

References

[1] S. Moro, V. Teeda, D. Scazzoli, L. Reggiani, and M. Magarini, “Experimental UAV-aided RSSI localization of a ground RF emitter in 865 MHz and 2.4 GHz bands,” in *2022 IEEE 95th Vehicular Technology Conference:(VTC2022-Spring)*. IEEE, 2022, pp. 1–6.

[2] A. Masood *et al.*, “Surveying pervasive public safety communication technologies in the context of terrorist attacks,” *Phys. Commun.*, vol. 41, p. 101109, 2020.

[3] S. Tang *et al.*, “Study on RSS/AOA hybrid localization in life detection in huge disaster situation,” *Natural Hazards*, vol. 95, pp. 569–583, 2019.

[4] F. Maurelli, S. Krupiński, X. Xiang, and Y. Petillot, “AUV localisation: a review of passive and active techniques,” *Inter. J. Intell. Robotics Appl.*, pp. 1–24, 2021.

[5] H. P. Mistry and N. H. Mistry, “RSSI based localization scheme in wireless sensor networks: a survey,” in *Proc. 5th Int. Conf. Adv. Comput. Commun. Technol.* IEEE, 2015, pp. 647–652.

[6] B. Xiang *et al.*, “UAV assisted localization scheme of WSNs using RSSI and CSI information,” in *Proc. Int. Conf. Comput. Commun.*, 2020, pp. 718–722.

[7] M. Hasanzade *et al.*, “Localization and tracking of RF emitting targets with multiple unmanned aerial vehicles in large scale environments with uncertain transmitter power,” in *Int. Conf. Unmanned Aircraft Syst.*, 2017, pp. 1058–1065.

[8] S. Shue, L. E. Johnson, and J. M. Conrad, “Utilization of XBee ZigBee modules and MATLAB for RSSI localization applications,” in *Proc. SoutheastCon*, 2017, pp. 1–6.

[9] G. Wang, H. Chen, Y. Li, and N. Ansari, “NLOS error mitigation for TOA-based localization via convex relaxation,” *IEEE Trans. Wireless Commun.*, vol. 13, pp. 4119–4131, 2014.

[10] Y. Liu, F. Guo, L. Yang, and W. Jiang, “An improved algebraic solution for TDOA localization with sensor position errors,” *IEEE Commun. Lett.*, vol. 19, no. 12, pp. 2218–2221, 2015.

[11] H.-J. Shao, X.-P. Zhang, and Z. Wang, “Efficient closed-form algorithms for AOA based self-localization of sensor nodes using auxiliary variables,” *IEEE Trans. Signal Process.*, vol. 62, pp. 2580–2594, 2014.

[12] S. M. M. Dehghan, H. Moradi, and S. A. A. Shahidian, “Optimal path planning for DRSSI based localization of an RF source by multiple uavs,” in *Proc. RSI/ISM Int. Conf. Robot. Mechatronics*, 2014, pp. 558–563.

[13] S. Nagaraju, L. J. Gudino, B. V. Kadam, R. Ookalkar, and S. Udeshi, "RSSI based indoor localization with interference avoidance for wireless sensor networks using anchor node with sector antennas," in *Proc. Int. Conf. Wireless Commun. Signal Proc. Netw.*, 2016, pp. 2233–2237.

[14] D. Konings *et al.*, "The effects of interference on the RSSI values of a ZigBee based indoor localization system," in *Proc. Int. Conf. Mechatronics Mach. Vision Pract.*, 2017, pp. 1–5.

[15] X. Jiang, N. Li, Y. Guo, W. Xie, and J. Sheng, "Multi-emitter localization via concurrent variational bayesian inference in uav-based wsn," *IEEE Communications Letters*, vol. 25, no. 7, pp. 2255–2259, 2021.

[16] L. K. Dressel and M. J. Kochenderfer, "Efficient and low-cost localization of radio signals with a multirotor UAV," in *Proc. AIAA Guidance, Navig. Control Conf.*, 2018, p. 1845.

[17] M. Petitjean, S. Mezhoud, and F. Quitin, "Fast localization of ground-based mobile terminals with a transceiver-equipped UAV," in *Proc. 29th Int. Symp. Pers. Indoor Mob. Radio Commun.*, 2018, pp. 323–327.

[18] Analog Devices Inc, "PlutoSDR Wiki Page," [Online]. Available:: https://wiki.analog.com/university/tools/pluto, accessed: 07/10/2023.

[19] Fraunhofer HHI, "QuaDRiGa Channel Model Homepage," [Online]. Available:: https://quadriga-channel-model.de/, accessed: 07/10/2023.

[20] Z. Yu, Z. Liu, F. Meyer, A. Conti, and M. Z. Win, "Localization based on channel impulse response estimates," in *2020 IEEE/ION Position, Location and Navigation Symposium (PLANS)*. IEEE, 2020, pp. 1014–1021.

[21] X. Sun, C. Wu, X. Gao, and G. Y. Li, "Fingerprint-based localization for massive MIMO-OFDM system with deep convolutional neural networks," *IEEE Transactions on Vehicular Technology*, vol. 68, no. 11, pp. 10 846–10 857, 2019.

[22] J. Zhang, L. Liu, Y. Fan, L. Zhuang, T. Zhou, and Z. Piao, "Wireless channel propagation scenarios identification: A perspective of machine learning," *IEEE Access*, vol. 8, pp. 47 797–47 806, 2020.

[23] T. Van Nguyen, Y. Jeong, H. Shin, and M. Z. Win, "Machine learning for wideband localization," *IEEE Journal on Selected Areas in Communications*, vol. 33, no. 7, pp. 1357–1380, 2015.

[24] G. Wainer, M. Aloqaily *et al.*, "Machine learning-based indoor localization and occupancy estimation using 5G ultra-dense networks," *Simulation Modelling Practice and Theory*, vol. 118, p. 102543, 2022.

[25] Y. Zhong, F. Wu, J. Zhang, and B. Dong, "Wifi indoor localization based on k-means," in *2016 International Conference on Audio, Language and Image Processing (ICALIP)*. IEEE, 2016, pp. 663–667.

[26] K. F. P. Wye, E. Kanagaraj, S. M. M. S. Zakaria, L. M. Kamarudin, A. Zakaria, K. Kamarudin, and N. Ahmad, "RSSI-based localization zoning using k-mean clustering," in *IOP Conference Series: Materials Science and Engineering*, vol. 705, no. 1, 2019, p. 012038.

[27] Z. Li, A. Giorgetti, and S. Kandeepan, "Multiple radio transmitter localization via UAV-based mapping," *IEEE Transactions on Vehicular Technology*, vol. 70, no. 9, pp. 8811–8822, 2021.

[28] Z. M. Livinsa and S. Jayashri, "Performance analysis of diverse environment based on RSSI localization algorithms in WSNs," in *2013 IEEE Conference on Information & Communication Technologies*. IEEE, 2013, pp. 572–576.

[29] R. J. Rossi, *Mathematical statistics: an introduction to likelihood based inference*. John Wiley & Sons, 2018.

[30] A. Patri and S. P. Rath, "Elimination of Gaussian noise using entropy function for a RSSI based localization," in *Proc. Intern. Conf. Image Inf. Process.*, 2013, pp. 690–694.

[31] C. M. Judd, G. H. McClelland, and C. S. Ryan, *Data analysis: A model comparison approach*. Routledge, 2011.

[32] R. O. Duda, P. E. Hart *et al.*, *Pattern classification and scene analysis*. Wiley New York, 1973, vol. 3.

[33] P. Bholowalia and A. Kumar, "EBK-means: A clustering technique based on elbow method and k-means in WSN," *International Journal of Computer Applications*, vol. 105, no. 9, 2014.

[34] M. Saelens *et al.*, "Impact of EU duty cycle and transmission power limitations for sub-GHz LPWAN SRDs: An overview and future challenges," *Eurasip J. Wirel. Commun. Netw.*, pp. 1–32, 2019.

[35] Texas Instrument, "Low-cost low-power 2.4 GHz RF transceiver," [Online]. Available: https://bit.ly/3Ct9yvf, accessed: 9/3/2021.

[36] H. Sallouha, M. M. Azari, and S. Pollin, "Energy-constrained UAV trajectory design for ground node localization," in *Proc. IEEE GLOBECOM*, 2018, pp. 1–7.

[37] D. Ebrahimi, S. Sharafeddine, P.-H. Ho, and C. Assi, "Autonomous UAV trajectory for localizing ground objects: A reinforcement learning approach," *IEEE Transactions on Mobile Computing*, vol. 20, no. 4, pp. 1312–1324, 2021.

[38] Raspberry Pi Foundation, "SenseHat Board," [Online]. Available: https://www.raspberrypi.org/products/sense-hat/, accessed: 07/10/2023.

[39] U-blox, "GPS Dongle Documentation," [Online]. Available: https://bit.ly/3LR6peS, accessed: 07/10/2023.